Reversible plastic events during oscillatory deformation of amorphous solids

Nikolai V. Priezjev
Department of Mechanical and Materials Engineering, Wright State University, Dayton, Ohio 45435, USA
(Received 28 October 2015; published 6 January 2016)

The effect of oscillatory shear strain on nonaffine rearrangements of individual particles in a three-dimensional binary glass is investigated using molecular dynamics simulations. The amorphous material is represented by the Kob-Andersen mixture at the temperature well below the glass transition. We find that during periodic shear deformation of the material, some particles undergo reversible nonaffine displacements with amplitudes that are approximately power-law distributed. Our simulations show that particles with large amplitudes of nonaffine displacement exhibit a collective behavior; namely, they tend to aggregate into relatively compact clusters that become comparable with the system size near the yield strain. Along with reversible displacements there exist a number of irreversible ones. With increasing strain amplitude, the probability of irreversible displacements during one cycle increases, which leads to permanent structural relaxation of the material.

DOI: 10.1103/PhysRevE.93.013001

I. INTRODUCTION

Understanding the structure-property relationship of amorphous polymers and metallic glasses is important for many technological and biomedical applications [1,2]. The mechanism of plastic deformation in amorphous materials involves an accumulation of highly localized structural rearrangements of atoms or the so-called shear transformation zones [3–5]. It was recently demonstrated that in sheared glasses a strong correlation exists between a collective rearrangement of small groups of atoms and quasilocalized soft modes, or "soft spots," which are analogous to dislocations in crystalline solids [6–10]. Molecular dynamics (MD) simulations suggest that specific atomic packing configurations with the most unfavorable local coordination polyhedra are more likely to participate in soft spots in metallic glasses [10,11]. Furthermore, a local plastic event in sheared amorphous solids induces long-range deformation that in turn might trigger secondary events and give rise to avalanches [12]. In related studies, it was shown that a local reversible shear transformation in a quiescent system results in cage jumps (discrete events where particles escape from cages of their neighbors) whose density is larger in the cases of weakly damped dynamics or slow shear transformation [13,14].

In recent years, the mechanical response of amorphous materials to cyclic shear was examined experimentally [15–23] by means of molecular dynamics simulations [24–31] and continuum modeling [32]. It was shown that at strain amplitudes below a critical value, particle trajectories are reversible after either one or several cycles, and the diffusion is suppressed [15,21,24–27,29]. In contrast, at larger strain amplitudes, the number of cage breaking events increases, and the particle dynamics becomes spatially and temporally heterogeneous [16,24,25,28,29]. However, the nature of the transition (a sharp crossover versus a continuous nonequilibrium phase transition [20,23,30]) and its relation to chaotic behavior [26] remain not fully understood.

In the previous MD studies of binary [25] and polymeric [28] glasses under oscillatory shear strain, the structural relaxation was studied by analyzing the self-overlap order parameter and the dynamic susceptibility. It was found that at small strain amplitudes, the system dynamics is nearly reversible during several thousands of oscillation periods. On the other hand, at strain amplitudes above the critical value, the memory of the initial state is lost during several cycles, and a large fraction of particles undergo irreversible displacements [25,28]. Remarkably, it was shown that at the critical strain amplitude that separates slow and fast relaxation dynamics, the number of particles involved in a correlated motion reaches maximum [25,28]. Furthermore, the cage-breaking events were identified from a sequence of particle positions at the end of each cycle and studied at different strain amplitudes. In particular, it was demonstrated that dynamic facilitation of mobile particles by their neighbors becomes increasingly pronounced at larger strain amplitudes [25,28]. However, the analysis of particle displacements in the previous studies did not include plastic rearrangements that occur during a single oscillation cycle.

In this paper, the structural relaxation process in a binary glass under cyclic loading is investigated using molecular dynamics simulations. We find that while the system dynamics at small strain amplitudes is reversible after each cycle, most particles undergo nonaffine displacements with amplitudes that are broadly distributed. Moreover, the results of numerical simulations indicate that large nonaffine rearrangements are spatially heterogeneous, with the typical length scale on the order of the system size near the yield strain.

The rest of the paper is structured as follows. The molecular dynamics simulation model and the deformation protocol are described in the next section. The analysis of nonaffine displacements of particles at different strain amplitudes is presented in Sec. III. Brief conclusions are provided in the final section.

II. DETAILS OF MOLECULAR DYNAMICS SIMULATIONS

We perform molecular dynamics simulations of a binary (80:20) Lennard-Jones (LJ) glass model, which was first introduced by Kob and Andersen [33]. The three-dimensional system consists of $N = 10\,000$ particles placed in a periodic box as illustrated in Fig. 1. In this model, any two particles $\alpha,\beta = A,B$ interact via the LJ potential, which is

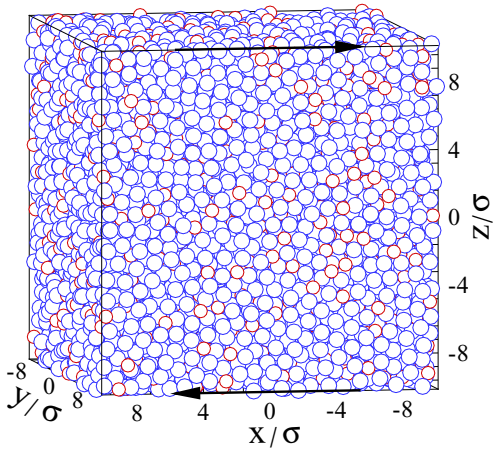

FIG. 1. A snapshot of an equilibrated binary LJ glass that is subject to oscillatory shear strain in the xz plane (indicated by solid arrows). Atoms of type A are denoted by large blue circles and type B by small red circles. The Lees-Edwards periodic boundary conditions are applied in the xz plane.

defined as

$$V_{\alpha\beta}(r) = 4\varepsilon_{\alpha\beta}\left[\left(\frac{\sigma_{\alpha\beta}}{r}\right)^{12} - \left(\frac{\sigma_{\alpha\beta}}{r}\right)^{6}\right], \quad (1)$$

where the parameters are set as $\varepsilon_{AA} = 1.0$, $\varepsilon_{AB} = 1.5$, $\varepsilon_{BB} = 0.5$, $\sigma_{AB} = 0.8$, $\sigma_{BB} = 0.88$, and $m_A = m_B$ [33]. The cutoff radius is $r_{c,\alpha\beta} = 2.245\sigma_{\alpha\beta}$. In what follows, the units of length, mass, energy, and time are set as $\sigma = \sigma_{AA}$, $m = m_A$, $\varepsilon = \varepsilon_{AA}$, and $\tau = \sigma\sqrt{m/\varepsilon}$, respectively. The simulations were carried out at a constant density $\rho = \rho_A + \rho_B = 1.2\sigma^{-3}$ in a cubic box of linear size $L = 20.27\sigma$. Newton's equations of motion were solved numerically using the fifth-order Gear predictor-corrector integration scheme [34] with a time step $\triangle t_{MD} = 0.005\tau$.

The system was initially equilibrated in the absence of shear at the temperature $1.1\ \varepsilon/k_B$, which is well above the glass transition temperature $T_g \approx 0.45\ \varepsilon/k_B$ [33]. Here k_B is the Boltzmann constant. Then, the temperature was gradually reduced with the rate of $10^{-5}\ \varepsilon/k_B\tau$ to the final temperature $T = 10^{-2}\ \varepsilon/k_B$. After additional 5×10^6 MD steps, the periodic shear strain was applied in the xz plane according to

$$\gamma(t) = \gamma_0 \sin(\omega t), \quad (2)$$

where ω is the oscillation frequency and γ_0 is the strain amplitude. The simulations were carried out with the oscillation frequency $\omega\tau = 0.001$ and, correspondingly, the period $T = 2\pi/\omega = 6283.19\tau$. In our study, the shear deformation was implemented using the SLLOD algorithm [35] combined with the Lees-Edwards periodic boundary conditions in the xz plane. The constant temperature of the system was maintained by rescaling the $\hat{y}$ component of the velocity for each particle. In addition, periodic boundary conditions were applied along the $\hat{y}$ direction (perpendicular to the plane of shear). After discarding several cycles, the positions of all particles were saved every $T/12 = 523.60\tau$ during fifty oscillation periods. The data were accumulated in eight independent samples for each strain amplitude.

III. RESULTS

The local plastic event in sheared amorphous materials can be detected by computing nonaffine displacements of particles with respect to its neighbors [4]. We first evaluate the transformation matrix $\mathbf{J}_i$ that best maps all bonds between a particle i and its nearest neighbors at times t and $t + \Delta t$. The nonaffine displacement of the particle i is computed as follows:

$$D^2(t,\Delta t) = \frac{1}{N_i}\sum_{j=1}^{N_i}\{\mathbf{r}_j(t+\Delta t) - \mathbf{r}_i(t+\Delta t) - \mathbf{J}_i[\mathbf{r}_j(t) - \mathbf{r}_i(t)]\}^2, \quad (3)$$

where the sum is taken over the neighboring atoms within the radius $r_c = 1.5\sigma$ from the position vector $\mathbf{r}_i(t)$ [10,11]. In our study, the time lag Δt was varied in the range from $T/12$ to $50T$. Note also that the oscillation period was chosen so that the time interval between consecutive particle configurations, $T/12 = 523.60\tau$, is much larger than the typical timescale of irreversible rearrangements of particles [4].

The probability distribution function of the quantity D^2 for different strain amplitudes is presented in Fig. 2. The data were collected in bins $0.001\sigma^2$ at the time lag $\Delta t = T/4$ and time $t = 0$. It can be observed in Fig. 2 that at strain amplitudes $\gamma_0 \leqslant 0.07$, most of the particles undergo affine displacements characterized by small values $D^2 \lesssim 0.004\sigma^2$. At the same time, however, the displacement of some particles deviates significantly from a linear strain field, and the quantity D^2 becomes relatively large. The tails of the probability distribution functions are approximately power-law distributed with a slope of the decay approaching -2 at the strain amplitude $\gamma_0 = 0.07$. Thus, the threshold for the local plastic

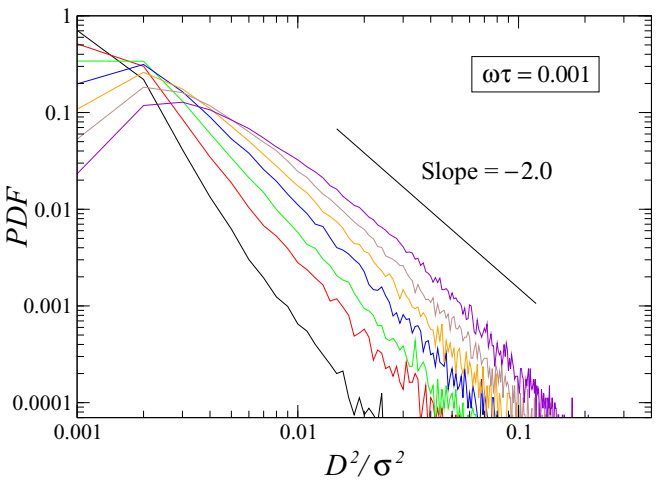

FIG. 2. The normalized probability distribution function of $D^2(t,\Delta t)$ defined by Eq. (3) for the strain amplitudes $\gamma_0 =$ 0.01,0.02,0.03,0.04,0.05,0.06, and 0.07 (from left to right). The quantity $D^2(t,\Delta t)$ was measured at $t = 0$ and $\Delta t = T/4$, where T is the oscillation period. The straight line with the slope -2 is plotted for reference.

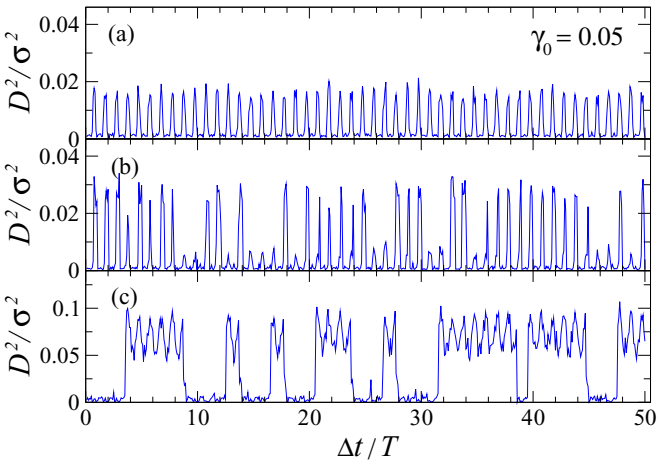

FIG. 3. Variation of $D^2(0,\Delta t)$ as a function of the time lag Δt for three particles during 50 periods at the strain amplitude $\gamma_0 = 0.05$ and oscillation frequency $\omega\tau = 0.001$. Note that the vertical scale in panel (c) is different.

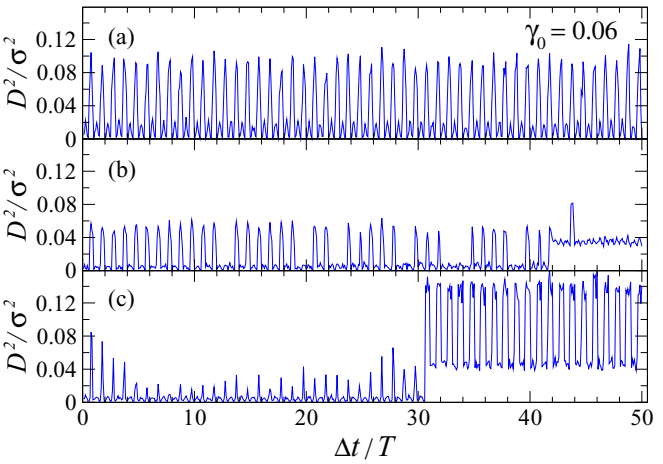

FIG. 4. The dependence of the quantity $D^2(0,\Delta t)$ as a function of the time lag Δt for three different particles at the strain amplitude $\gamma_0 = 0.06$ and oscillation frequency $\omega\tau = 0.001$.

deformation is somewhat arbitrary, and in what follows, we define it to be $D^2 = 0.01\sigma^2$. Similarly, a small fraction of the atomic size was chosen as a critical value of D in the previous MD studies of actively deformed metallic glasses [10,36]. Note also that the definition of D^2 in Eq. (3) involves averaging over changes in the nearest-neighbor distances, and, therefore, the threshold $D^2 = 0.01\sigma^2$ is consistent with the value 0.1σ used to define cage jumps in the previous studies on oscillatory shear deformation of binary glasses [13,16,25].

Figure 3 shows the variation of the quantity D^2 as a function of the time lag Δt for selected particles at the strain amplitude $\gamma_0 = 0.05$. We compare particle configurations separated by the time interval Δt with respect to $t = 0$. It can be seen in Fig. 3(a) that the displacement of the particle can be well described by the affine transformation during the first half of each cycle, while it undergoes large nonaffine displacements during the second half of each cycle. Notice that the function $D^2(0,\Delta t)$ is periodic with superimposed noise, possibly because of the thermal fluctuations. We find, however, that local nonaffine displacements are not always periodic. For example, as shown in Fig. 3(b), the particle undergoes large nonaffine displacements separated by periods with relatively small amplitudes of nonaffine displacements. We comment that this behavior is different from completely repetitive limit cycles observed in athermal quasistatic simulations [26,27].

Furthermore, on rare occasions, we detect particles that temporarily escape the cage of their neighbors while still undergoing periodic nonaffine displacements [see Fig. 3(c)]. This behavior is consistent with the observation of reversible cage jumps during oscillatory shear deformation of a binary glass, where particle trajectories were analyzed using the cage detection algorithm [25]. It was also found that irreversible cage jumps typically occur after 10^2–10^3 cycles at the strain amplitude $\gamma_0 = 0.05$ and frequency $\omega\tau = 0.02$, when the root mean square displacement of particles becomes comparable with the cage size [25]. As a reminder, the critical strain amplitude $\gamma_0 = 0.06$ marks the transition from a slow dynamics with a broad subdiffusive plateau to a diffusive regime governed by irreversible displacements of particles [25]. Finally, examples of repetitive nonaffine displacements at the strain amplitude $\gamma_0 = 0.06$ are shown in Fig. 4 for three particles. It can be seen that during 50 oscillation periods, the displacements are reversible except for the time lags $\Delta t \approx 42T$ in Fig. 4(b) and $\Delta t \approx 31T$ in Fig. 4(c), when sudden irreversible rearrangements take place.

Typical configurations of particles with large nonaffine displacements ($D^2 > 0.01\sigma^2$) after a quarter of a cycle are presented in Fig. 5 for the strain amplitudes $0.02 \leqslant \gamma_0 \leqslant 0.05$. It is evident from Fig. 5(a) that even at the small strain amplitude $\gamma_0 = 0.02$, these particles form relatively large, compact clusters as well as a few isolated clusters that consist only of a few atoms. With increasing strain amplitude, the

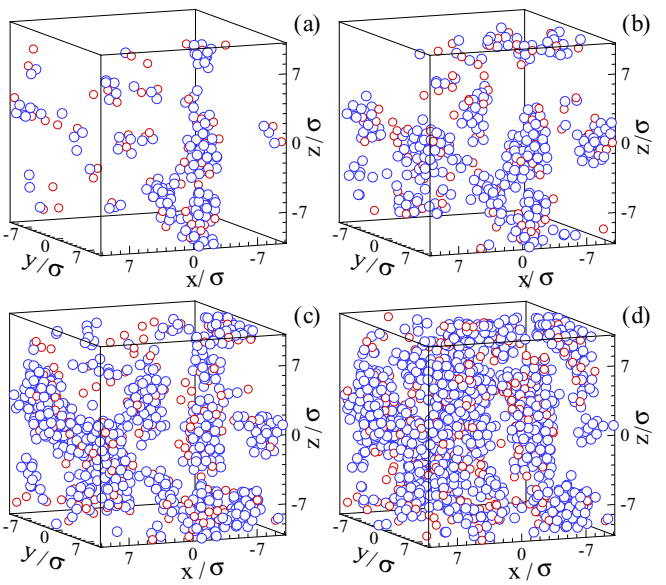

FIG. 5. The positions of particles of type A (large blue circles) and particles of type B (small red circles) at the shear strain $\gamma(t = T/4) = \gamma_0$ and $D^2(0,T/4) > 0.01\sigma^2$ for the strain amplitudes (a) $\gamma_0 = 0.02$, (b) $\gamma_0 = 0.03$, (c) $\gamma_0 = 0.04$, and (d) $\gamma_0 = 0.05$.

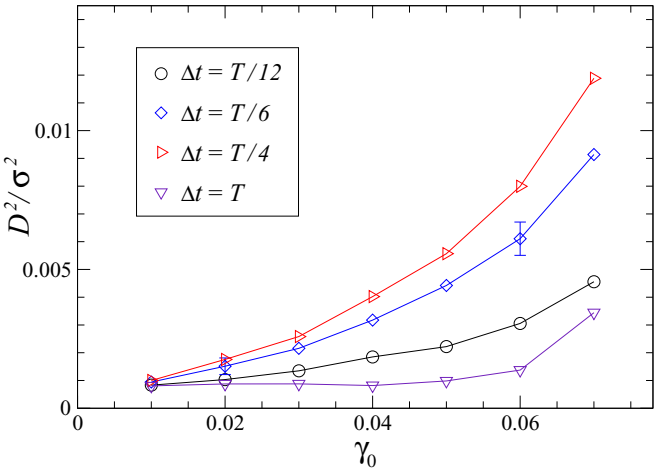

FIG. 6. The averaged quantity $D^2(0,\Delta t)$ as a function of the strain amplitude γ_0 for the time lags $\Delta t = T/12$ (○), $T/6$ (◇), $T/4$ (▷), and T (▽), where T is the oscillation period. The shear strain $\gamma(t)$ at $t = \Delta t$ is given by Eq. (2).

cluster size increases and becomes comparable with the system size at $\gamma_0 \geqslant 0.04$. Thus, we identify a *dynamical process* that involves a correlated motion of particles and leads to percolation of nonaffine displacements at sufficiently large strain amplitudes. Note that snapshots of particles shown in Figs. 5(a)–5(d) were taken in the same sample, and, therefore, the clusters at different strain amplitudes appear to be spatially correlated. We also mention that the cluster size distribution was not computed in our study because of the limited statistics. Since only a few large clusters per sample are formed, and these clusters are nearly reversible over fifty cycles, it is expected that a reliable cluster size distribution can be obtained by averaging over a larger number of independent samples (e.g., 10^3 instead of 8). Interestingly, a power-law distribution of energy drops below yield strain was recently reported in a model 2D solid subject to oscillatory quasistatic shear [31].

The dependence of the quantity $D^2(0,\Delta t)$ as a function of the strain amplitude is plotted in Fig. 6 for different time lags Δt, which determine shear strain according to Eq. (2). The nonaffine displacements were averaged over all particles in eight independent samples with respect to $t = 0$. It appears that at the smallest strain amplitude $\gamma_0 = 0.01$, the difference in $D^2(0,\Delta t)$ for various time lags in Fig. 6 is barely noticeable, because only a small fraction of particles undergo large nonaffine displacements (see Fig. 2). As expected, the average of $D^2(0,\Delta t)$ increases with increasing shear strain $\gamma(\Delta t)$, and it becomes greater than $0.01\sigma^2$ at the maximum strain $\gamma(T/4) = \gamma_0 = 0.07$. Note also that $D^2(0,T)$ after a full back-and-forth cycle is not zero, which implies that relative positions of a particle and its nearest neighbors are not exactly reversible even at small strain amplitudes due to thermal motion of particles within their cages. This is consistent with the results shown in Fig. 3. Furthermore, the relatively large increase of $D^2(0,T)$ at the strain amplitudes $\gamma_0 = 0.06$ and 0.07 in Fig. 6 reflects the occurrence of irreversible displacements after a single cycle. These results confirm that with increasing strain amplitude above $\gamma_0 = 0.06$, the number of irreversible cage jumps after one cycle increases, and the root mean square displacement of particles becomes greater than the cage size [25]. These conclusions also agree with the definition of the yielding transition that occurs at the largest strain amplitude below which the microstructure is reversible [18].

IV. CONCLUSIONS

In summary, molecular dynamics simulations were conducted to study structural relaxation in a three-dimensional model glass submitted to periodic shear. We considered the Kob-Andersen binary mixture at the temperature which is well below the glass transition. The nonaffine component of the particle displacement was evaluated during multiple time intervals with respect to the system configuration at zero strain. It was found that even at strain amplitudes below yield, some particles undergo large nonaffine displacements that are reversible after each cycle. The magnitudes of the nonaffine displacement, computed after a quarter of a cycle, are approximately power-law distributed with the slope that depends on the strain amplitude. During cyclic loading, mobile particles tend to aggregate into transient clusters which become larger with increasing strain amplitude. The probability of irreversible rearrangements after a full cycle also increases, leading to permanent structural relaxation of the material at large strain amplitudes.

ACKNOWLEDGMENTS

Financial support from the National Science Foundation (CNS-1531923) is gratefully acknowledged. The author would like to thank I. Regev for useful comments. Computational work in support of this research was performed at Michigan State University's High Performance Computing Facility and the Ohio Supercomputer Center.

[1] J. C. Qiao and J. M. Pelletier, J. Mater. Sci. Technol. **30**, 523 (2014).
[2] T. Voigtmann, Curr. Opin. Colloid Interface Sci. **19**, 549 (2014).
[3] A. S. Argon, Acta Metall. **27**, 47 (1979).
[4] M. L. Falk and J. S. Langer, Phys. Rev. E **57**, 7192 (1998).
[5] P. Schall, D. A. Weitz, and F. Spaepen, Science **318**, 1895 (2007).
[6] A. Tanguy, B. Mantisi, and M. Tsamados, Europhys. Lett. **90**, 16004 (2010).
[7] M. L. Manning and A. J. Liu, Phys. Rev. Lett. **107**, 108302 (2011).
[8] S. S. Schoenholz, A. J. Liu, R. A. Riggleman, and J. Rottler, Phys. Rev. X **4**, 031014 (2014).
[9] A. Tanguy, JOM **67**, 1832 (2015).
[10] J. Ding, S. Patinet, M. L. Falk, Y. Cheng, and E. Ma, Proc. Natl. Acad. Sci. USA **111**, 14052 (2014).
[11] J. Ding, Y. Q. Cheng, and E. Ma, Appl. Phys. Lett. **101**, 121917 (2012).
[12] A. Lemaitre and C. Caroli, Phys. Rev. Lett. **103**, 065501 (2009).
[13] N. V. Priezjev, Phys. Rev. E **91**, 032412 (2015).
[14] N. V. Priezjev, J. Phys.: Condens. Matter **27**, 435002 (2015).

[15] M. Lundberg, K. Krishan, N. Xu, C. S. O'Hern, and M. Dennin, Phys. Rev. E **77**, 041505 (2008).
[16] R. Candelier, O. Dauchot, and G. Biroli, Phys. Rev. Lett. **102**, 088001 (2009).
[17] S. Slotterback, M. Mailman, K. Ronaszegi, M. van Hecke, M. Girvan, and W. Losert, Phys. Rev. E **85**, 021309 (2012).
[18] N. C. Keim and P. E. Arratia, Soft Matter **9**, 6222 (2013).
[19] K. E. Jensen, D. A. Weitz, and F. Spaepen, Phys. Rev. E **90**, 042305 (2014).
[20] E. D. Knowlton, D. J. Pine, and L. Cipelletti, Soft Matter **10**, 6931 (2014).
[21] N. C. Keim and P. E. Arratia, Phys. Rev. Lett. **112**, 028302 (2014).
[22] M. C. Rogers, K. Chen, L. Andrzejewski, S. Narayanan, S. Ramakrishnan, R. L. Leheny, and J. L. Harden, Phys. Rev. E **90**, 062310 (2014).
[23] K. H. Nagamanasa, S. Gokhale, A. K. Sood, and R. Ganapathy, Phys. Rev. E **89**, 062308 (2014).
[24] D. Fiocco, G. Foffi, and S. Sastry, Phys. Rev. E **88**, 020301(R) (2013).
[25] N. V. Priezjev, Phys. Rev. E **87**, 052302 (2013).
[26] I. Regev, T. Lookman, and C. Reichhardt, Phys. Rev. E **88**, 062401 (2013).
[27] C. F. Schreck, R. S. Hoy, M. D. Shattuck, and C. S. O'Hern, Phys. Rev. E **88**, 052205 (2013).
[28] N. V. Priezjev, Phys. Rev. E **89**, 012601 (2014).
[29] M. Mailman, M. Harrington, M. Girvan, and W. Losert, Phys. Rev. Lett. **112**, 228001 (2014).
[30] T. Kawasaki and L. Berthier, arXiv:1507.04120.
[31] I. Regev, J. Weber, C. Reichhardt, K. A. Dahmen, and T. Lookman, Nat. Commun. **6**, 8805 (2015).
[32] N. Perchikov and E. Bouchbinder, Phys. Rev. E **89**, 062307 (2014).
[33] W. Kob and H. C. Andersen, Phys. Rev. E **51**, 4626 (1995).
[34] M. P. Allen and D. J. Tildesley, *Computer Simulation of Liquids* (Clarendon, Oxford, 1987).
[35] D. J. Evans and G. P. Morriss, *Statistical Mechanics of Nonequilibrium Liquids* (Academic Press, London, 1990).
[36] H. L. Peng, M. Z. Li, and W. H. Wang, Phys. Rev. Lett. **106**, 135503 (2011).